ChemComm

COMMUNICATION

View Article Online
View Journal | View Issue

Cite this: *Chem. Commun.*, 2022, **58**, 10520

Received 16th March 2022,
Accepted 23rd August 2022

DOI: 10.1039/d2cc01520j

rsc.li/chemcomm

Efficient covalent capping of carbon and gold with TEMPO for catalysis and spin writing†‡

Vitalijs Romanovs,*[a] Valery Sidorkin,*[b] Evgeniya Doronina[b] and Viatcheslav Jouikov*[c]

Covalent immobilization of TEMPO at carbon and gold *via* an aliphatic $-(CH_2)_6-$ linker was achieved *via* cathodic grafting of a diamagnetic precursor, tetramethylpiperidine, with subsequent >NH to >NO oxidation to give TEMPO-capped paramagnetic interfaces (Γ_{TEMPO} = 5.2 × 10^{-10} mol cm^{-2}); catalytic and spin switching potential of the thus prepared systems was demonstrated.

Immobilization of 2,2,6,6-tetramethyl piperidyl oxide (TEMPO) stable radicals at solid conducting supports is a key element in a large number of applications[1–3] related to interfaces with permanent magnetic character that are sought for sensing,[4] electronic,[5,6] energy storage,[6–11] catalysis,[12–18] biomedical,[11,19] and other fields. Two critical issues are to be dealt with here: (i) simple and reliable immobilization/fixation of TEMPO at the support and (ii) a long, chemically stable and atom-economical spacer attaching TEMPO to the support.

Covalent grafting of TEMPO is obviously more advantageous than its mechanical incorporation into composites because of its much smaller consumption, reducing the thickness of the immobilized phase to a monolayer, avoiding its leakage from the interface and providing better solvent and mechanical stability.[5,8,16] While diamagnetic substrates can be easily grafted *via* their diazonium derivatives,[20] the radical character of TEMPO excludes this radical-based process.[5] However, the cationic nitroxonium form of TEMPO obtained through its disproportionation in an acid medium can be grafted from its diazonium derivative and subsequently reduced back to a nitroxyl radical by cathodic cycling.[5]

Non-radical covalent immobilizations of TEMPO at carbons and CNTs were also reported,[8,21–23] with a common drawback being a specific pre-treatment of the substrate or precursor, while the resulting "scaffold" is either excessively bulky or chemically non-inert.

When a well-shaped EPR response of the grafted radical centers is required for operating their spin states,[24] a sufficiently long spacer separating them from the surface is needed to prevent masking their EPR signal by surface electronic conductivity.[10,23–26] A relatively long linker is as well required to enable a pseudo-diffusional behavior of the immobilized radical units,[27] which is critical for catalytic applications. Due to their chemical inertness, flexibility and smaller footprints on the surface compared to those of TEMPO itself, alkyl linkers appear most advantageous for this purpose.

We report here on a simple and efficient covalent attachment of TEMPO to carbonaceous and gold interfaces using non-diazonium alternative grafting[28,29] *via* an aliphatic linker $(CH_2)_n$ (n = 6) preserving the redox reactivity and distinct EPR response of TEMPO.

An easy to handle diamagnetic precursor of TEMPO fitted with a $(CH_2)_6$ linker has been prepared from commercially available 4-hydroxy-2,2,6,6-tetramethyl-piperidine (TMP-OH) and 1-bromo-6-chloro-hexane (ESI†) (Scheme 1), chosen because of its moderately long alkyl chain and availability.

Nucleophilic grafting of TMP-O$(CH_2)_6$I to carbonaceous supports was realized *via* an S_N2-like process upon their activation[29] by scanning between −1.5 and −2.0 V *vs.* Ag/AgCl (Fig. 1) until total blocking of the electrode by the grafted units.

Note that the polarity of CH_3CN is not high enough to allow a one-electron reduction of the C–I bond of the hexyl linker,[30] thus excluding the radical grafting pathway. Various carbonaceous supports were functionalized this way: bulky glassy carbon (GC) and CG cloth, HOPG, natural Ceylon graphite, technical graphite rods and an HB pencil lead.

For a covalent attachment of the TMP precursor to Au, spontaneous *in situ* formation of oxidative addition intermediate

[a] *Latvian Institute of Organic Synthesis, LV-1006 Riga, Latvia. E-mail: vitalijs.romanovs@inbox.lv*
[b] *A. E. Favorsky Irkutsk Institute of Chemistry, 664033 Irkutsk, Russia. E-mail: svf@irioch.irk.ru*
[c] *UMR 6226 ISCR, University of Rennes 1, 35042 Rennes, France. E-mail: vjouikov@univ-rennes1.fr*

† This paper is dedicated to Prof. Jacques Simonet for his significant contribution in the fields of organic electrochemistry and surface functionalization.

‡ Electronic supplementary information (ESI) available: Synthetic details, EIS at TMP and TMP·HCl interfaces, EDS data for the TEMPO-grafted gold interface, and oscillograms of redox switching $TEMPO^+$/TEMPO grafted onto graphite. See DOI: https://doi.org/10.1039/d2cc01520j

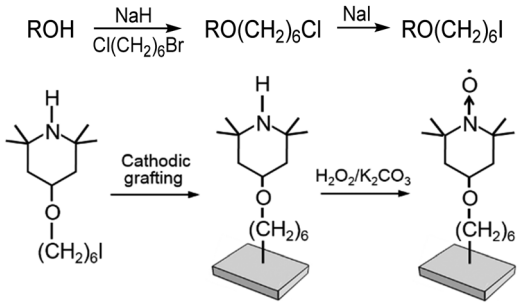

Scheme 1 Synthesis (R = 4-TMP), immobilization of TMP-O$(CH_2)_6$I and oxidation of the grafted N–H functions to N→O.

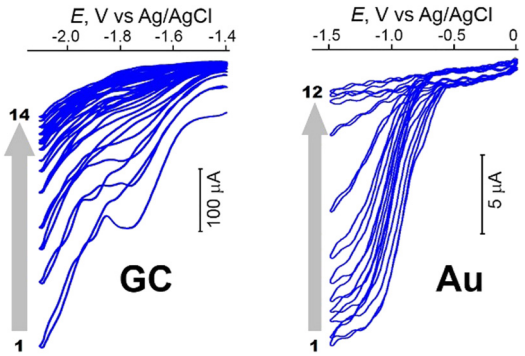

Fig. 1 Cathodic grafting of TMP-O$(CH_2)_6$I onto GC (14 consecutive scans from −1.4 to −2.1 V) and gold (12 scans from 0 to −1.5 V). CH_3CN/0.1 M Bu_4NPF_6, ν = 50 mV s^{-1}. T = 293 K.

TMP-O$(CH_2)_6$–Au(II)-I and its one-electron reduction (Fig. 1) at moderate cathodic potentials ($E \cong -1$ V)[24,28] were exploited. A similar procedure can be used for Pt (Fig. S1, ESI†), Ag and Cu as well.

The thus prepared GC and Au interfaces both show an irreversible signal (E_p = 1.18 V) of oxidation of TMP units (Fig. 2A). Its integration (Q = 3.62 μC for an electrode of ∅ = 3 mm) provides an estimate of their efficient surface concentration as Γ_∞(TMP) ≅ 5.2×10^{-10} mol cm^{-2}. This value is surprisingly close to that found for TEMPO thiol-attached to gold *via* a $(CH_2)_{15}$C(O)NH linker (4.6×10^{-10} mol cm^{-2} [26]) and is two times higher than the coverage of an ideally flat surface at a 90% maximal hexagonal packing (2.7×10^{-10} mol cm^{-2}). Apparent maximal coverage at GC is Γ_∞(TMP) ≅ 5.4×10^{-9} mol cm^{-2}, approaching that observed for grafting Fc$(CH_2)_6$ onto GC (10×10^{-9} mol cm^{-2} [30]). Since nucleophilic grafting specifically provides a single layer coverage, these high values evidently stem from the roughness of the GC interface.

After oxidizing the grafted TMP units by dipping into the H_2O_2/K_2CO_3 solution (ESI†), the interface shows a reversible peak of a TEMPO$^+$/TEMPO redox pair (E_o = 0.69 V) whose coulometry attests to a quantitative TMP to TEMPO conversion (Fig. 2B). In CH_3CN/0.1 M Bu_4NPF_6 solution, the immobilized redox couple TEMPO$^+$/TEMPO is quite stable upon repetitive cycling (Fig. 2B–D); cyclic voltammetry and two-step potentiostatic chronoamperometry (at E_p) show no visible diminishing

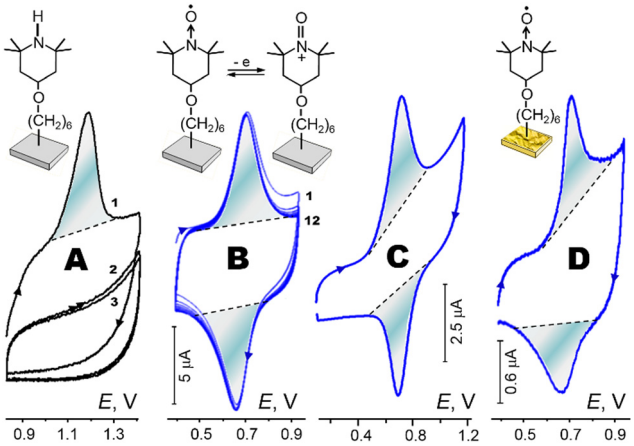

Fig. 2 Voltammetry of the grafted interfaces. (A) Three anodic cycles at a GC electrode: irreversible oxidation of the grafted TMP units. (B) Same electrode (12 cycles) after converting TMP to TEMPO with H_2O_2/K_2CO_3; reversible oxidation of TEMPO. (C) TEMPO-capped HOPG. (D) TEMPO-capped Au. CH_3CN/0.1 M Bu_4NPF_6, ν = 50 mV s^{-1}. T = 293 K. The shadowed zones show current integration.

of the amount of immobilized TEMPO (after $> 10^5$ cycles, see Fig. S3, ESI†).

The FTIR reflection spectra of the grafted GC interfaces before and after peroxide oxidation (Fig. 3D) show the disappearance of the characteristic N–H vibration modes (3360, 700 cm^{-1}) and the appearance of the band of N → O (960 cm^{-1}). The SEM images of the grafted interface (Fig. 3A–C) show smoothening of the micro relief of the bare GC surface by the immobilized layers, while EDS atom analysis attests to the presence of C, N and O atoms at the gold interface (Fig. S4, ESI†).

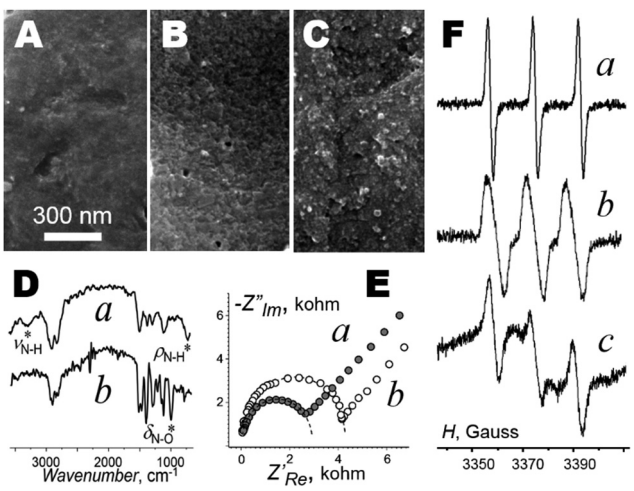

Fig. 3 The SEM images of the GC surface: (A) before grafting, (B) after immobilization of 4-hexyloxy-piperidine and (C) after the oxidation of the grafted TMP to TEMPO. (D) The FTIR reflectance spectra of the GC interface functionalized with (a) TMP and (b) TEMPO. (E) The Nyquist plots for the reduction of chloranil at (a) TMP and (b) TEMPO capped interfaces, E_o = −0.1 V, f = 0.24 MHz to 0.1 Hz. ΔE = 10 mV (see also Fig. S2, ESI†). (F) The EPR spectra of TEMPO covalently grafted *via* an O$(CH_2)_6$ linker to: (a) GC, (b) a bundle of GC fibres, and (c) 0.5 mm HB pencil lead.

The $(CH_2)_6$O-TMP-covered GC interface is EPR silent but upon its oxidation with H_2O_2, a distinct well-resolved triplet (Fig. 3F) of TEMPO appears (g = 2.006, a_N = 15 G); similar spectra were obtained with a TEMPO-grafted HOPG stripe and 0.5 mm HB pencil lead. Using a bundle of *ca.* 30 GC fibers (5.56 μm in diameter) functionalized with $(CH_2)_6$O-TEMPO and fixing the static field at the central line of the nitrogen spectrum (H = 3374 G), the word "SPIN" (Fig. 4) was written in Morse code switching between paramagnetic and diamagnetic states of the interface by on-off polarization steps (E = 0.2 V for ON and E = 1.2 V for OFF states). Note that in contrast to the interface with redox-switchable *n*-propyl-linked silatranyl radicals,[24] the paramagnetic state corresponds here to lower voltage, so the spin writing with TEMPO is rather a "spin-erasing" technique with a stationary spin-ON state (for permanent redox-switching of TEMPO/TEMPOL couple, see (Fig. S5, ESI†)).

The thus prepared TEMPO-modified interfaces were probed for catalytic alcohol oxidation, one of the major applications of TEMPO.[12–18,31–33] The voltammetric responses of a gold $(CH_2)_6$O-TEMPO-capped interface (in CH_3CN/0.1 M Bu_4NPF_6) in the presence of $PhCH_2OH$ (0.02 mol L^{-1}) and 2,6-lutidine (0.08 mol L^{-1}) used as a base well show all characteristic features of a catalytic process: increase of the current with respect to the response of the catalyst in the absence of the alcohol (Fig. 5A–C), disappearance of the reverse current of the reversible redox pair of the catalyst; and, seen for sharper shaped voltammograms (Fig. 5B), a backward kinetic shift of the oxidation peak because of fast consumption of the active form of the catalyst (N═O$^+$ cation) in a follow up catalytic reaction. The efficiency of recovery of the nitroxyl radical (Fig. 5A) due to high turnover of the catalytic reaction with the alcohol ($i_p^{cat} \cong 7.5 \times i_p^{TEMPO}$) is close to that of TEMPO thiol-attached to Au nano particles.[31] For comparison, under homogeneous conditions (C_{TEMPO} = 7 mmol L^{-1} in CH_3CN), this i_p^{cat}/i_p ratio was only attained with a 100× excess of $PhCH_2OH$.[32,33]

In aqueous alkali media (pH 10), the catalytic feature at the TEMPO-functionalized Au electrode is more complex (Fig. S5, ESI†),

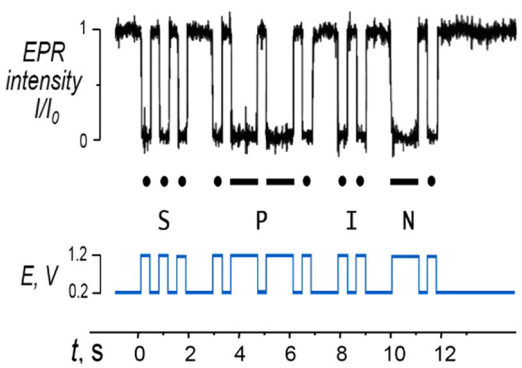

Fig. 4 Commutation of the EPR response of the TEMPO$^+$/TEMPO redox couple immobilized at GC fibres (∅ 5 μm): the word "SPIN" written in inverted-key Morse code. Spin switching commands: E_{OFF}("0") = 1.2 V, E_{ON}("1") = 0.2 V, static field 3374 Gauss, and modulation amplitude 2 G. T = 293 K.

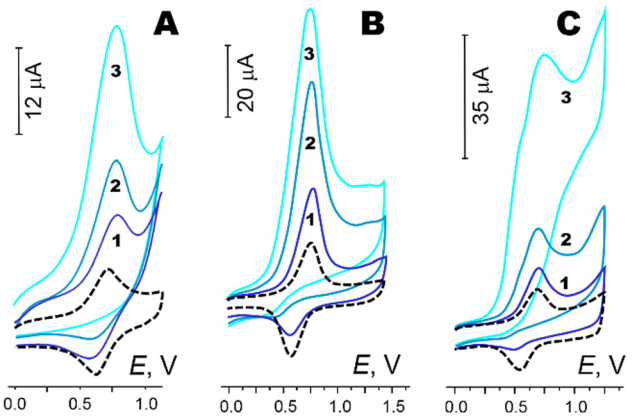

Fig. 5 Catalysis of the oxidation of benzyl alcohol by the immobilized couple TEMPO$^+$/TEMPO. (A) TEMPO-capped Au electrode in CH_3CN/0.1 M Bu_4NPF_6 + 2,6-lutidine (0.08 mol L^{-1}) without (broken line) and in the presence (solid) of $PhCH_2OH$: (1) 5, (2) 10, and (3) 30 mmol L^{-1}, ν = 250 mV s^{-1}. (B and C) TEMPO-capped (B) GC and (C) graphite paste electrodes in H_2O/K_2CO_3 (pH 10) in the presence of $PhCH_2OH$: (1) 2, (2) 4 and (3) (*B*: 5 mmol L^{-1}, *C*: 20 mmol L^{-1}), ν = 100 mV s^{-1}. T = 293 K.

which is yet to be entirely rationalized (see Fig. S6, ESI†). Under the same conditions, the responses of TEMPO-modified graphitic electrodes (Fig. 5B and C), more suitable for large scale catalytic oxidations,[16] show a rapid loss of the reversibility of the N═O$^+$/NO$^•$ system, while the catalytic current increases with the concentration of $PhCH_2OH$, in line with the previous reports.[16,31–34] It is to be noted that with an excellent proper stability of the grafted TEMPO layer (see Fig. S3, ESI†), its partial degradation occurs during large scale alcohol oxidation due to undesired side reactions of TEMPO, also reported in other works.[16,31]

Thus, the cathodic covalent functionalization of various carbon and gold interfaces with TEMPO using a universal aliphatic linker, equally suitable for both supports, was shown to be very advantageous in terms of easily available precursors (including those with different CH_2 chain lengths), a very simple experimental protocol and good grafting efficiency. This method provides an excellent stability of TEMPO-functionalized interfaces; with this, an easy and deliberate CH_2-incremental variation of the length of the attaching spacer and hence the thickness of the underlying hydrophobic layer is possible, allowing the creation of interfaces with promising properties for spin-commutation, catalysis and other applications. Further work on immobilized radical systems is under progress.

The authors are grateful to European PostDoc Latvia #1.1.1.2/VIAA/3/19/577 (V. R.) and PHC OSMOSE Project no: 48362YK (V. R. and V. J.) for financial support.

Conflicts of interest

The authors have no conflicts to declare.

References

1 J. E. Nutting, M. Rafiee and S. S. Stahl, *Chem. Rev.*, 2018, **118/9**, 4834–4885.
2 Z. Zhou and L. Liu, *Curr. Org. Chem.*, 2014, **18/4**, 459–474.

3 A. Das and S. S. Stahl, *Angew. Chem., Int. Ed.*, 2017, **56**/**30**, 8892–8897.
4 S. Abdellaoui, K. L. Knoche, K. Lim, D. P. Hickey and S. D. Minteer, *J. Electrochem. Soc.*, 2016, **163**/**4**, H3001–H3005.
5 C. Cougnon, S. Boisard, O. Cador, M. Dias, E. Levillain and T. Breton, *Chem. Commun.*, 2013, **49**, 4555–4557.
6 H. Nishide and K. Oyaizu, *Science*, 2008, **319**, 737–738.
7 K. Koshika, N. Sano, K. Oyazu and H. Nishide, *Chem. Commun.*, 2009, 836–838.
8 E. Lebegue, T. Brousse, J. Gabicher, R. Retoux and C. Cougnon, *J. Mater. Chem. A*, 2014, **2**, 8599–8602.
9 X. Wei, W. Xu, M. Vijayakumar, L. Cosimbescu, T. Liu, V. Sprenkle and W. Wang, *Adv. Mater.*, 2014, **26**, 7649–7653.
10 T. Suga, H. Ohshiro, S. Sugita, K. Oyaizu and H. Nishide, *Adv. Mater.*, 2009, **21**, 1627–1630.
11 G. I. Likhtenshtein, J. Yamauchi, S. Nakatsuji, A. I. Smirnov and R. Tamura, Nitroxides Applications in Chemistry, *Biomedicine, and Materials Science*, Wiley-VCH, Weinheim, 2008.
12 X. Yi, S. Lei, W. Liu, F. Che, C. Yu, X. Liu, Z. Wang, X. Zhou and Y. Zhang, *Org. Lett.*, 2020, **22**/**12**, 4583–4587.
13 R. A. Sheldon, I. W. C. E. Arends, G.-J. T. Brink and A. Dijksman, *Acc. Chem. Res.*, 2002, **35**, 774.
14 R. Ciriminna, G. Palmisano and M. Pagliaro, *ChemCatChem*, 2015, **7**, 552–558.
15 A. Kipke, K. U. Schöning, M. Yusubov and A. Kirschning, *Eur. J. Org. Chem.*, 2017, 6906–6913.
16 F. Geneste, C. Moinet, S. Ababou-Girard and F. Solal, *New J. Chem.*, 2005, **29**, 1520–1526.
17 A. Michaud, G. Gingras, M. Morin, F. Bland, R. Ciriminna, D. Avnir and M. Pagliaro, *Org. Process Res. Dev.*, 2007, **11**, 766–768.
18 R. Ciriminna and M. Pagliar, *Org. Process Res. Dev.*, 2010, **14**, 245–251.
19 A. Hirohata, K. Yamada, Y. Nakatani, I.-L. Prejbeanu, B. Diény, P. Pirro and B. Hillebrands, *J. Magn. Magn. Mater.*, 2020, **509**, 166711.
20 M. M. Chehimi, Aryl Diazonium Salts, *New Coupling Agents in Polymer and Surface Science*, Wiley-VCH Verlag & Co. KGaA, Weinheim, Germany, 2012.
21 W. Choi, S. Endo, K. Oyaizu and H. Nishide, *J. Mater. Chem. A*, 2013, **1**, 2999–3003.
22 D. Q. Fan, J. P. He, W. Tang, J. T. Xu and Y. L. Yang, *Eur. Polym. J.*, 2007, **43**, 26–34.
23 M. Gilhespy, M. Lok and X. Baucherel, *Catal. Today*, 2006, **117**, 114–119.
24 C. Peureux and V. Jouikov, *Chem. – Eur. J.*, 2014, **20**, 9357–9366.
25 Z. Wilamowski, M. Solnica, E. Michaluk, M. Havlicek and W. Jantsch, *Semicond. Sci. Technol.*, 2011, **26**/**6**, 064009.
26 P. Krukowski, W. Kozlowski, W. Olejniczak, Z. Klusek, M. Puchalski, P. Dabrowski, P. J. Kowalczyk, K. Gwozdzinski and G. Grabowski, *Appl. Surf. Sci.*, 2008, **255**, 1921–1928.
27 P.-Y. Blanchard, O. Alévêque, T. Breton and E. Levillain, *Langmuir*, 2012, **28**, 1371–1374.
28 V. Jouikov and J. Simonet, *J. Appl. Electrochem.*, 2012, **42**/**7**, 527–537.
29 V. Jouikov and J. Simonet, *Langmuir*, 2012, **28**/**1**, 931–938.
30 J. Simonet and V. Jouikov, *Electrochem. Commun.*, 2014, **38**, 65–67.
31 O. Swiech, R. Bilewicz and E. Megie, *RSC Adv.*, 2013, **3**, 5979–5986.
32 A. C. Herath and J. Y. Becker, *Electrochim. Acta*, 2008, **53**, 4324–4330.
33 M. Rafiee, B. Karimi and S. Alizadeh, *ChemElectroChem*, 2014, **1**, 455–462.
34 R. A. Green, J. T. Hill-Cousins, R. C. D. Brown, D. Pletcher and S. G. Leach, *Electrochim. Acta*, 2013, **113**, 550–556.